Korean J. Chem. Eng., **27**(3), 836-842 (2010)
DOI: 10.1007/s11814-010-0166-y

Evaluation of direct formic acid fuel cells with catalyst layers coated by electrospray

Yongchai Kwon*, Seungmin Baek, Byungwan Kwon**, Jinsoo Kim**, and Jonghee Han***,†**

*Department of Chemical and Environmental Technology, Inha Technical College,
253, Yonghyun-dong, Nam-gu, Incheon 402-752, Korea
**Department of Chemical Engineering, Kyung Hee University,
1 Seocheon-dong, Giheung-gu, Yongin, Gyeonggi-do 446-701, Korea
***Fuel Cell Research Center, KIST, 39-1 Hawolgok-dong, Seongbuk-gu, Seoul 130-650, Korea
(*Received 7 September 2009 • accepted 16 November 2009*)

Abstract−We investigated cell performance and performed phenomenological analyses of direct formic acid fuel cells (DFAFCs) incorporating anode (palladium) and cathode (platinum) catalysts prepared using a new electrospray coating technique. To optimize the design of the DFAFC, we examined the cell performance by the Pd catalyst loading and formic acid feed rate. Of Pd catalyst loaded samples, 3 mg/cm^2 sample showed the highest electrical performance with formic acid feed rate of 5 ml/min. This behavior was caused by discrepancies in the mass transfer limitation. When the feed rate was greater than 10 mL/min, however, the 7 mg/cm^2 sample provided the highest electrical performance, which was attributed to enhanced electrooxidation reactions. For comparison of the effect of the catalyst coating method on the cell performance of DFAFC, polarization curves of the DFAFC incorporating catalysts prepared using a conventional airspray coating method were also measured. As a result of the comparison, the electrospray coating-used DFAFC showed better cell performance. Based on these results, the cell performance of the DFAFCs was optimized when the catalysts using the electrospray catalyst coating were employed, the amount of Pd loaded on the anode electrode was 3 mg/cm^2 (Pd thickness: ~6 μm), and the formic acid feed rate was 10 mL/min.

Key words: Direct Formic Acid Fuel Cell, Electrospray, Mass Transfer, Electrooxidation

INTRODUCTION

There is considerable interest at present in developing miniaturized fuel cell systems for use as battery replacements in various consumer and military electronic devices [1-8]. Miniaturized fuel cell systems make it easy to store a high energy density and to quickly recharge fuel cartridges. Among the plausible fuel cell systems, direct methanol fuel cells (DMFCs) have attracted much attention [2,7-10], but their drawbacks-including (1) low catalyst activity for the oxidation of methanol at room temperature and (2) high methanol crossover causing decrease in the mixed potential of cathode, (3) poisoning of the cathode catalyst, and (4) reduced cell efficiency-have limited their realization [9,11] In particular, the high crossover of methanol restricts the exploitation of high-concentration methanol solutions, which would be desirable for affordable portable power applications. It is generally believed that the usable concentration range of methanol is less than 2 M [3].

The use of direct formic acid fuel cells (DFAFCs), which use direct liquid formic acid as a fuel to generate power, overcomes most of the difficulties associated with DMFCs [4-6,12-21]. The crossover in a DFAFC is lower than that in a DMFC by two orders of magnitude because of the anionic effect of formic acid, thereby allowing its use at relatively high concentrations. DFAFCs also provide up to a sixfold higher power density than do DMFCs, thereby allowing them to be operated at room temperature [11]. In addition, the theoretical electromotive force (EMF) of formic acid, estimated from the Gibbs free energy, is high (1.45 V) [1], meaning that it possesses a highly activated reaction capability. Because of these advantageous features, interest in DFAFCs is soaring.

Critical aspects toward improving the performance and cost-efficiency of DFAFCs include the selection of the anode catalyst material and optimization of the loading of the expensive noble metal catalyst. In this respect, palladium (Pd)-based catalysts are becoming more important than conventionally used platinum (Pt)-based catalysts because they suffer less CO poisoning, resulting in higher kinetic activities and lower costs (Pd is cheaper than Pt by a factor of five) [22-24].

Pd catalysts are conventionally sprayed by hand spray, i.e., the so-called "air spray" method. However, because the "hand spray" method sprays catalyst using compressed air, there are drawbacks like the large size of distributed liquid aerosol and the large loss of catalyst to the atmosphere [25].

To overcome these difficulties during device fabrication, in this study we used a new catalyst coating technique, the "electrospray" method [26-28]. This approach employs a fine liquid aerosol created through an electrostatic charging effect. After passing through a nozzle, the resulting film droplets of the reactant liquids are charged electrically under a high voltage. As more charge is added, the liquids in the nozzle become unstable, eventually reaching a critical point at which they do not absorb additional electrical charges, and at which point they spray in the form of tiny, highly charged droplets from the tip of the nozzle. These droplets will land on surfaces that possess the opposite charge [26,27]. Electrostatic repulsion between the charged particles impedes their agglomeration and promotes their adhesion with the substrate.

†To whom correspondence should be addressed.
E-mail: jhan@kist.re.kr

In this paper, we describe a new electrospray coating method for the fabrication of catalysts and its application to the preparation of DFAFCs. The optimal coating conditions were established through phenomenological analyses; the effects of the Pd catalyst loading and the formic acid feed rate on the DFAFC performance were then probed to establish its optimal design. In addition, we propose a phenomenological model that agrees well with the experimental results. It establishes a protocol for determining the optimal thickness of the catalyst layer loaded on the anode and provides critical information for elucidating the dominant mechanism underlying the performance of the DFAFC.

EXPERIMENTAL

The electrospray method was used to coat the catalysts in DFAFCs featuring a membrane and electrode assembly (MEA). The apparatus for electrospraying consisted of a high voltage supply, feeder, caterpillar tube, hot plate, and ground plate. Fig. 1 provides an approximate schematic representation of the apparatus used for the spraying of catalysts using the electrospray. The fuel cells were tested by using two types of noble metal catalysts: Pd and Pt. Palladium black catalyst (High Surface Area, Sigma-Aldrich) was employed for the anode; Pt black catalyst (HiSPEC™ 1000, Johnson Matthey) was employed for the cathode. The loading of the Pd catalyst upon the anode was a key parameter influencing the cell performance; herein, three different loadings were used: 1, 3, and 7 mg/cm^2. The loading of Pt catalyst upon the cathode was fixed at 4 mg/cm^2. Both Pd and Pt catalyst inks were prepared through initial mixing of catalyst powders with appropriate amounts of Millipore water, followed by mixing with appropriate amounts of 5% recast Nafion solution (1100EW, Solution Technology, Inc.), isopropyl alcohol, and 1-propanol.

The catalyst inks were sprayed, using the electrospraying method, onto the gas diffusion layer (GDL) attached to carbon paper (TGPH-060, Toray). The GDL was prepared through screen-printing of a slurry mixture consisting of carbon powder (Vulcan XC-72R, Carbot), Teflon emulsion (60%), and glycerol. After the anode and cathode electrodes were constructed, the pre-cleaned Nafion membrane (Nafion 115) was placed between them and then hot-pressed under a pressure of 1.7 tons at 140 °C for 5 min, to complete the manufacture of the MEA. The active area of the MEA was 3.2×3.2 cm^2. The area was used as the geometric area of electrode for evaluating the current densities as well as the active surface area of cyclic voltammetry (CV) tests. The MEA was then coupled with gas-sealing gaskets and placed between graphite blocks that had serpentine-like flow fields; finally, the liquid and gas reactants were fed into the graphite blocks. Prior to the cell polarization test, the MEA-included fuel cell configuration was subjected to a two-step pre-conditioning process, using a previously reported procedure [12]. During the first step, de-ionized (DI) water was fed into the fuel cell configuration at 95 °C for 1 h, and then the methanol-based cell polarization test was performed at 80 °C. During the test, 0.5 M methanol was fed into the anode while air was fed into the cathode; the feed rates were 5 mL/min and 500 sccm, respectively. The two-step pre-conditioning tests were conducted using a fuel cell testing station (Fuel Cell Control System, CNL, Inc.).

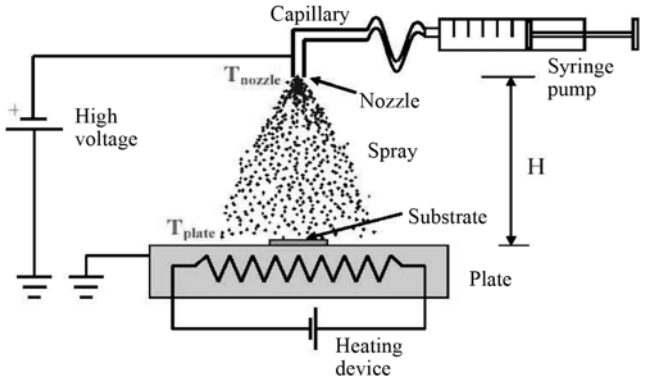

Fig. 1. Schematic representation of the electrospray coating process, with highly charged droplets sprayed from the tip of a nozzle.

The cell polarization tests with formic acid and air were performed in the same fuel cell testing station used for the pre-conditioning tests. Formic acid concentrations ranging from 5 to 15 M (increments of 5 M) were fed to the anode at a constant feed rate of 5 mL/min, while air (500 sccm) was provided to the cathode. All fuel cell tests were conducted at 30 °C. To estimate the electrochemically active surface (EAS) areas of the Pd catalysts on the anode electrode, CV tests were performed using a Solatron electrochemical workstation (FRA, Solartron 1260). DI water, acting as a working electrode, was introduced to the anode side at a flow rate of 5 mL/min, while hydrogen, serving as both a counter electrode and a dynamic hydrogen electrode (DHE), was introduced to the cathode at a flow rate of 200 sccm.

For the performance comparison, DFAFC incorporating anode (Pd) and cathode (Pt) catalysts prepared using airspray coating was manufactured and its performances were evaluated. The loading amounts of the Pd and Pt catalysts were 3 and 4 mg/cm^2, respectively. As for the loading procedure of catalysts, we used the same sequence that was reported elsewhere [29].

Scanning electron microscopy (SEM) and transmission electron microscopy (TEM) were used to measure the thickness and distribution, respectively, of the Pd catalyst after electrospraying.

RESULTS AND DISCUSSION

Figs. 2(a) and 2(b) display the effect of the loading of the Pd catalyst (1, 3, and 7 mg/cm^2) on the cell polarization curve. The formic acid concentration was 15 M and its feed rate was 5 mL/min. We chose such a high concentration of formic acid for these tests because it is more desirable for portable power applications [3,25]. When the loading of the Pd catalyst was 3 mg/cm^2, the cell activity was the highest; at 1 mg/cm^2, it was the lowest. It was initially expected that the cell activity at 7 mg/cm^2 Pd would be the highest because a larger EAS area (a larger number of the active reactive sites) affecting the cell activity was proportional to a larger loading of catalyst. As a plausible reason for an inconsistency between the conventional expectation (better cell activity in higher Pd loadings) and the actual experimental result (better cell activity in 3 mg/cm^2 than 7 mg/cm^2 Pd loading), a mass transport limitation occurring during the supply of formic acid to the anode is suggested. This effect was implicitly proved by the large drop in cell potential at the range

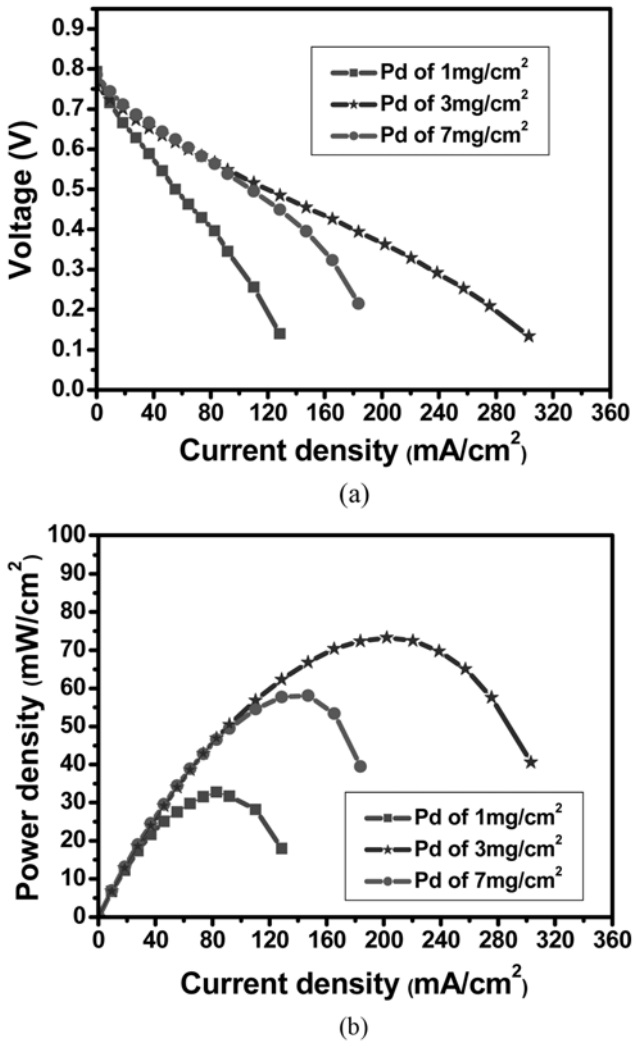

Fig. 2. Cell polarization curves plotted with respect to the loading of the Pd catalyst (1, 3, and 7 mg/cm^2); (a) V-I plot and (b) power density plot. The formic acid concentration was 15 M; the formic acid feed rate was 5 mL/min; the polarization tests were performed at 30 °C.

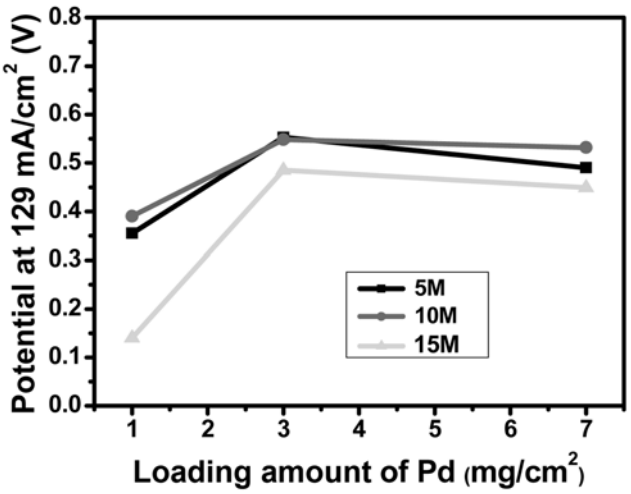

Fig. 3. Potentials measured at a fixed current density of 129 mA/cm^2, plotted with respect to the concentration of formic acid (5, 10, and 15 M) and the Pd catalyst loading (1, 3, and 7 mg/cm^2). The formic acid feed rate was 5 mL/min.

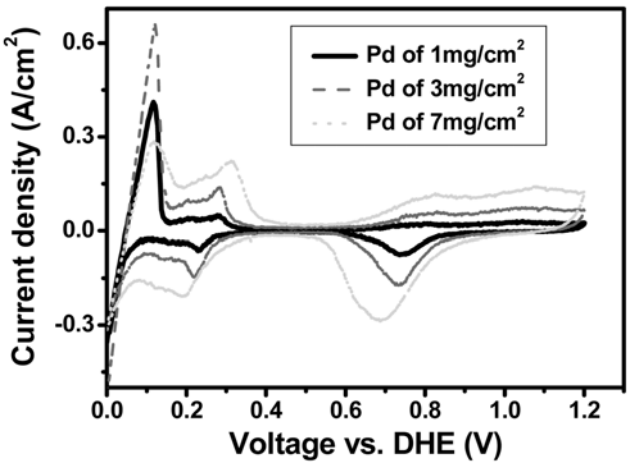

Fig. 4. Cyclic voltammograms of Pd catalysts loaded on anode electrodes at 1, 3, and 7 mg/cm^2; DI water flowing at the anode; H_2 flowing at the cathode.

of limiting current of the 7 mg/cm^2 Pd sample (the mass transport limitation effect is discussed below in further detail). Regarding power density (see Fig. 2(b)), the best maximum power density (74 mW/cm^2) was obtained for the 3 mg/cm^2 Pd sample.

Fig. 3 displays the effect of the formic acid concentration on the cell performance (potential) at various Pd catalyst loadings and 129 mA/cm^2. At all feed concentrations ranging from 5 to 15 M, the 3 mg/cm^2 Pd sample exhibited the highest potentials, meaning that the formic acid concentration did not considerably affect the link between the cell performance and the Pd loading.

The loading amount of Pd catalyst on the anode affects the EAS, which in turn influences the performance of the DFAFC [28,30, 31]. CV tests were performed using the samples with different Pd catalyst loadings and the results are shown in Fig. 4. As shown in Fig. 4, the area of the hydrogen desorption peak clearly increased with the Pd catalyst loading. In many cases, especially for Pt based catalysts, the area of hydrogen desorption peak can be translated directly to the EAS of the catalyst. However, the area of the hydrogen desorption peak of Pd based catalysts does not reflect the EAS exactly [25]. It is due to the hydrogen absorption capacity of Pd based materials. In the CV test of Pd catalysts, the hydrogen absorbed in Pd affects the hydrogen desorption reaction as following electrochemical oxidation: $H_{abs} \rightarrow H_{ads} \rightarrow H^+ + e^-$, where H_{abs} is the hydrogen absorbed into the Pd, while H_{ads} is the hydrogen adsorbed on the Pd surface [32]. Nevertheless, we may be able to qualitatively estimate the EAS of our samples from the CV tests by minimizing the effect of absorbed hydrogen on the electrochemical oxidation. To minimize the effect of absorbed hydrogen, we carried out exactly the same pretreatment procedure before the CV test. The same pretreatment procedure makes the compositions of the absorbed hydrogen in each sample to remain at the same level. Also, we introduced DI water instead of acid solution into the anode side in the CV test. This minimizes the hydrogen evolution (electrolysis of the

water occurs at 1.229 V [24] which is out of the potential range in the current CV test) and thus minimizes the hydrogen source for absorption. Owing to these experimental procedures, the amount of generated H_{abs} would be confined, although the loading in the Pd increases. Thereby, an increase in the Pd loading may lead to an increase in the electrochemical oxidation area of hydrogen, followed by an increase in the EAS of the Pd.

Based on the above results, it appears likely that limited mass transfer through diffusion loss was the main reason for the opposite trends between the cell activity and the loading of Pd catalyst, i.e., a lower amount of Pd catalyst (3 mg/cm^2) provided better cell performance than did a greater amount (7 mg/cm^2 sample). To verify and understand the "mass transfer" mechanism for diffusion loss in the DFAFCs, we examined the effect of the formic acid feed rate on the cell performance.

Figs. 5(a) and 5(b) display the effect of the feed rate (5, 10, or 12 mL/min) of 15 M formic acid on the cell polarization curves obtained for Pd loadings of 7 and 3 mg/cm^2, respectively. For the 7 mg/cm^2 Pd sample, we observe that as the feed rate of formic acid increased from 5 mL/min to greater than 10 mL/min, the large drop in cell potential at the range of limiting current density that we witnessed in Fig. 2(a) was alleviated considerably. On the other hand, for the 3 mg/cm^2 Pd sample, when compared with Fig. 2(a), there was little change in cell potential at the range of limiting current density upon increasing the feed rate of formic acid. Thus, the effect of the formic acid feed rate on the cell performance of the 3 mg/cm^2 Pd sample was trivial.

To further evaluate the effect of the formic acid feed rate on the DFAFC performance at various Pd loadings, we examined the potentials at 129 mA/cm^2 (Fig. 6(a)) and the maximum power densities (Fig. 6(b)) under the same conditions as those used to obtain Figs. 6(a) and 6(b). When the amount of Pd catalyst was 3 mg/cm^2, we observed no significant increases in either the potential at 129 mA/cm^2 or the maximum power density upon increasing the feed rate of formic acid (0.485 V and 73 mW/cm^2, at 5 mL/min; 0.499 V and 77 mW/cm^2, at 10 mL/min). Conversely, for the 7 mg/cm^2 Pd sam-

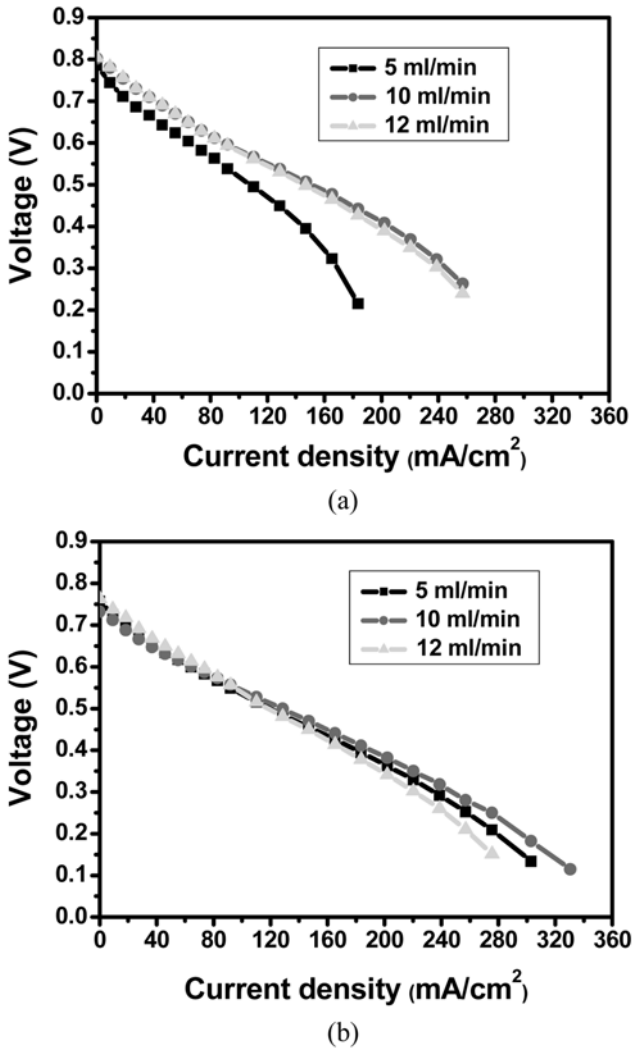

Fig. 5. Cell polarization curves plotted with respect to the feed rate (5, 10, and 12 mL/min) of 15 M formic acid at a fixed Pd loading; (a) Pd loading of 7 mg/cm^2 and (b) Pd loading of 3 mg/cm^2.

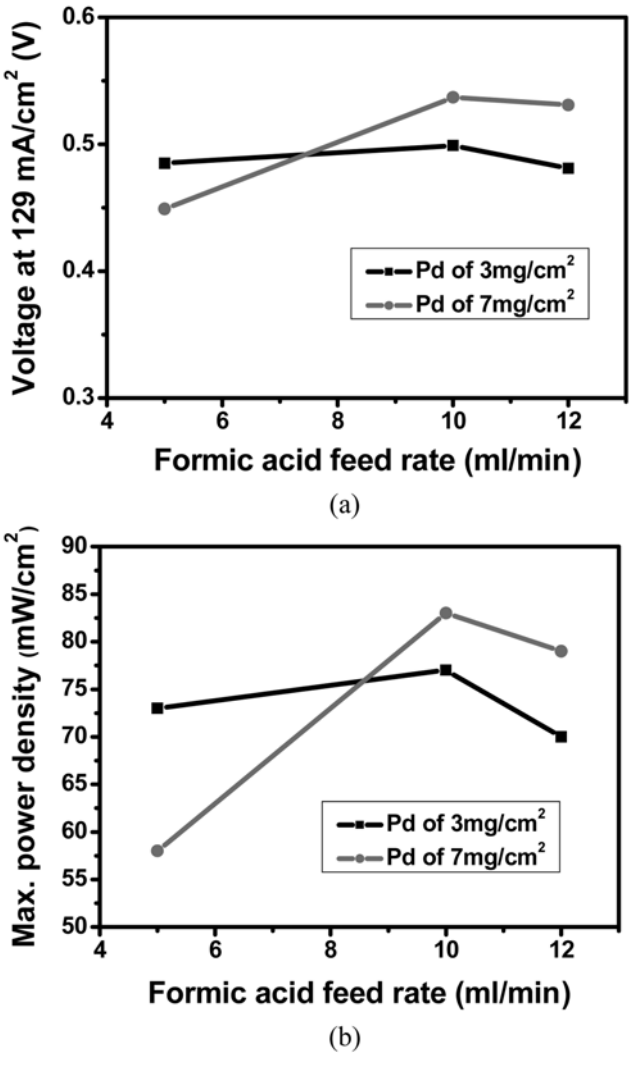

Fig. 6. (a) Potentials measured at a fixed current density of 129 mA/cm^2 and (b) maximum power densities plotted with respect to the feed rate (5, 10, and 12 mL/min) of 15 M formic acid and the Pd catalyst loading (3 and 7 mg/cm^2).

ple, these values increased appreciably upon increasing the feed rate (0.449 V and 58 mW/cm^2, at 5 mL/min; 0.537 V and 83 mW/cm^2, at 10 mL/min). The results in Figs. 5 and 6 were caused by discrepancies in the depletion rates of formic acid with the change in the formic acid feed rate when the formic acid passed the catalyst layer. The depletion rate of formic acid is generally dependent on the feed rate of formic acid (flowing speed (flux) of formic acid) and the thickness of the Pd catalyst layer being determined by the Pd loading [24].

The above phenomena can be explained by considering the following mechanism. When the formic acid feed rate was low (5 mL/min in this case), the depletion rate of formic acid appeared to be proportional to the loading of Pd catalyst because thickness of the Pd catalyst layer is expected to be proportional to the loading of Pd catalyst. Consequently, as the loading of the Pd catalyst layer decreased, formic acid was slowly depleted and its electrocatalytic reaction at the reactive interface remained active. Thus, the values of the power density and the potential at 129 mA/cm^2 for the 3 mg/cm^2 Pd sample were both higher than those for the 7 mg/cm^2 sample. When the formic acid feed rate increased (from 5 to 10 mL/min), however, the depletion rate of formic acid was retarded, irrespective of the loading (thickness) of the catalyst layer, because of its fast flow rate (high flux). Instead, the electrocatalytic reaction dominated the overall cell performance. As we have already explained, the electrocatalytic reaction depends on the number of active reaction sites, which is expected to be proportional to amount of catalyst loaded. Because changes in the dominant mechanism affected the cell performance, in this case the values of the power density and potential at 129 mA/cm^2 for the 7 mg/cm^2 Pd sample were higher than those for the 3 mg/cm^2 Pd sample.

With more increase in the formic acid feed rate (from 10 mL/min to 12 mL/min), the values of the power density and potential at 129 mA/cm^2 for the 7 mg/cm^2 Pd sample were higher than those for the 3 mg/cm^2 sample, although the differences in these values are not considerable. It was therefore understood that the formic acid feed rate of 12 mL/min was probably too fast to promote an electrocatalytic reaction, meaning it had odds that the formic acid contacted Pd catalyst layer intermittently [24]. When the formic acid feed rate was 15 mL/min, it seemed that the formic acid did not properly contact the Pd catalyst layer due to too fast speed. As a result, open circuit voltage (OCV) was degraded at fast rate and fuel cell operation did not even work.

From previous evaluation results, we recognized that it was necessary to estimate the correlation between the loading of the Pd catalyst and the catalyst layer thickness. The cross-sectional SEM images in Figs. 7(a)-7(f) reveal that samples possessing Pd loadings of 1, 3, and 7 mg/cm^2 had clearly distinguishable thicknesses in their Pd catalysts (ca. 2.5, 6, and 25 μm, respectively); the Pt catalyst layer on the cathode, loaded at 4 mg/cm^2, had a thickness of ca. 10 μm; the Nafion 115 electrolyte had a thickness of ca. 110 μm.

In addition to the layer thickness, measuring the particle sizes of the Pd catalysts is also a critical aspect determining whether the electrospray technique is a useful coating method for the preparation of DFAFCs. The TEM measurements in Fig. 8 reveal that the average size of the Pd nanoparticles in each sample was ca. 10 nm, with some sporadically displaced larger ones (>20 nm). These values are comparable with those obtained using the direct painting and hand spray methods [14].

For confirmation of the availability and superiority of the electrospray coating-used DFAFC structure, the polarization curves of

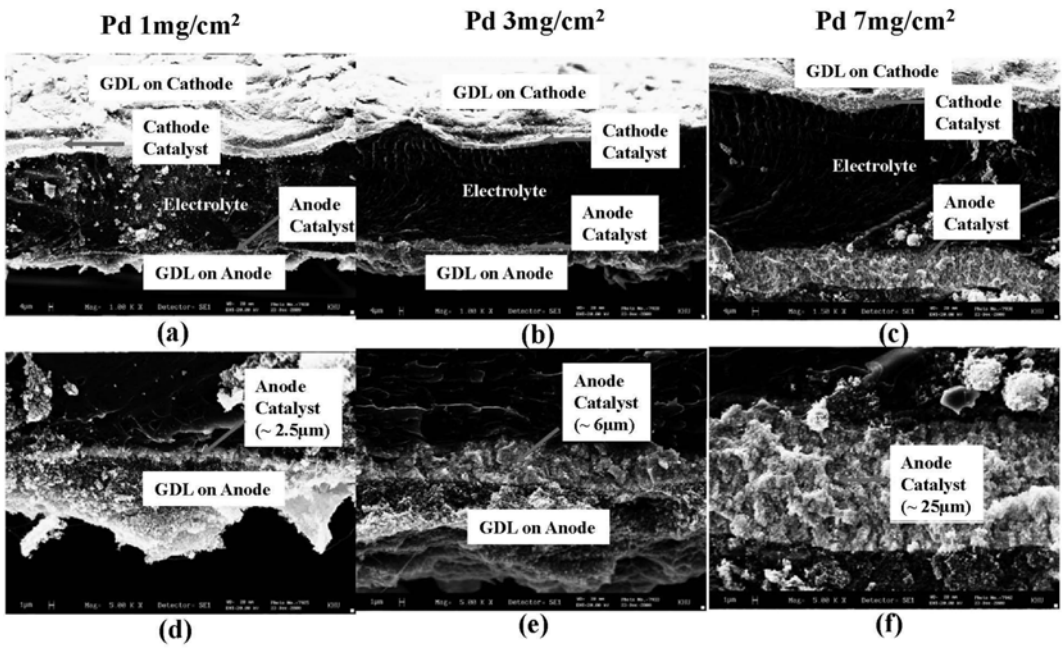

Fig. 7. Cross-sectional SEM images of Pd catalysts at three different loadings (1, 3, and 7 mg/cm^2) used to measure the thickness of each component of the MEA: (a)-(c) are the overall structure of MEA at three different Pd loadings (1, 3, and 7 mg/cm^2) and (d)-(f) are the enlarged images of the anode catalyst at three different Pd loadings (1, 3, and 7 mg/cm^2). The thicknesses of the Pd catalysts were ca. 2.5, ca. 6, and ca. 25 μm, respectively; the thickness of the cathode Pt catalyst, loaded at 4 mg/cm^2, was ca. 10 μm; the thickness of the Nafion 115 electrolyte was ca. 110 μm.

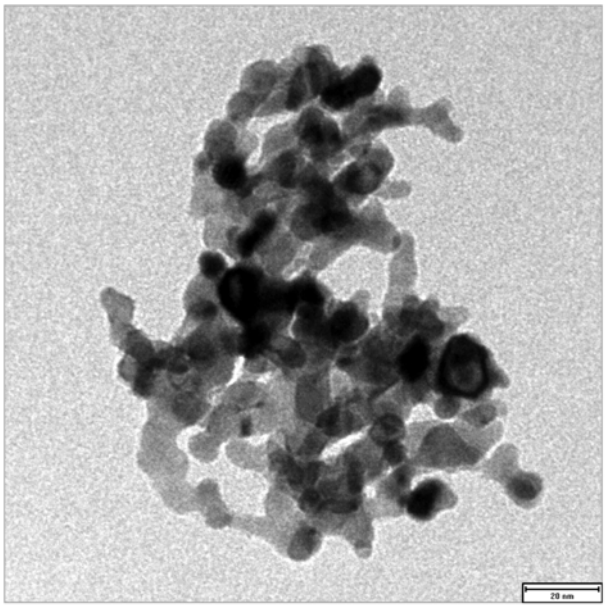

Fig. 8. TEM images of Pd catalyst samples loaded at 1, 3, and 7 mg/cm^2.

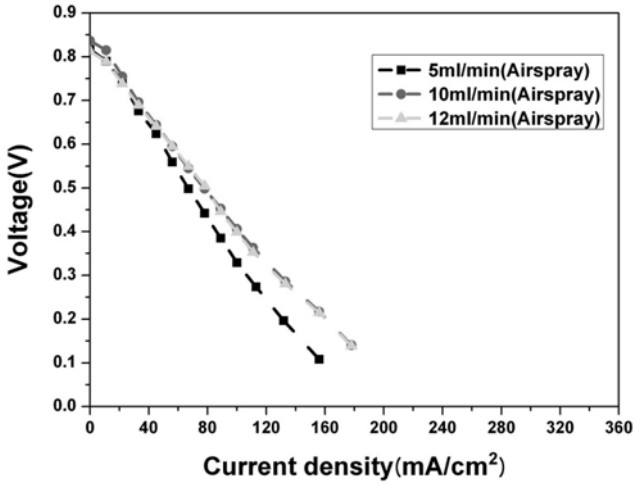

Fig. 9. Cell polarization curves plotted with respect to the feed rate (5, 10, and 12 mL/min) of 15 M formic acid at a fixed Pd loading of 3 mg/cm^2. The catalysts were sprayed by airspray coating method.

the airspray coating-used DFAFA that was performed under the same operational and formic acid fuel conditions as Fig. 5(a) were measured and the results presented in Fig. 9. When the effect of the catalyst coating method on the DFAFC polarization curve was compared between Fig. 5(a) and Fig. 9, the electrospray coating-used DFAFC showed better performance (the maximum power densities for the electrospray coating-used DFAFC were 73 mW/cm^2 at 5 mL/min, 77 mW/cm^2 at 10 mL/min, 68 mW/cm^2 at 12 mL/min while those for the airspray coating-used DFAFA were 34 mW/cm^2 at 5 mL/min, 41 mW/cm^2 at 10 mL/min, 39 mW/cm^2 at 12 mL/min).

Taking all of these results into consideration, we conclude that when the electrospray method is used, there is a threshold Pd loading required to form a suitably thick catalyst layer with which to obtain the optimal cell performance. In this case, a Pd loading of 3 mg/cm^2 provided a Pd catalyst thickness of ca. 6 μm and the best cell performance.

CONCLUSIONS

We have evaluated the cell performance and performed phenomenological analyses of DFAFCs manufactured using a new "electrospray" catalyst coating method. At a low formic acid feed rate (5 mL/min), a Pd catalyst loading of 3 mg/cm^2 provided a higher potential and power density than did the corresponding 7 mg/cm^2 sample. We attribute this difference to a loss of mass transfer by diffusion, where the depletion rate of formic acid was proportional to the loading of the catalyst layer. When the formic acid feed rate increased to >10 mL/min, however, we observed the opposite trend between the cell performance and the loading of the Pd catalyst; i.e., the 7 mg/cm^2 Pd catalyst sample exhibited a higher potential and power density than did the 3 mg/cm^2 sample. In this case, the effect of the formic acid depletion rate on the cell performance was weakened as a result of the faster feed speed of formic acid, whereas the rate of the electrocatalytic reaction, which depended on the loading of catalyst, increased. Taken together, we conclude that when the loading of Pd catalyst was between 3 and 7 mg/cm^2, the dominant factors affecting the cell performance were the loading itself and the feed rate of formic acid. For evaluating the effect of the catalyst coating method on the DFAFC polarization curve, the polarization curves of the electrospray coating-used DFAFC were compared with those of the airspray coating-used DFAFC and showed superior cell performance.

We eventually observed the best cell performance at a Pd loading of 3 mg/cm^2 Pd (i.e., a catalyst thickness ca. 6 μm).

ACKNOWLEDGMENTS

This work was supported by 2008 Inha Technical College Research Grant. The authors are grateful for the support from Inha Technical College.

REFERENCES

1. C. Rice, S. Ha, R. I. Masel, P. Waszczuk, A. Wieckowski and T. Barnard, *J. Power Sources*, **111**, 83 (2002).
2. X. Yu and P. G. Pickup, *J. Power Sources*, **182**, 124 (2008).
3. Y. Zhu, S. Ha and R. I. Masel, *J. Power Sources*, **130**, 8 (2004).
4. M. Neegat, T. Selier, E. R. Savinova and U. Stimming, *J. Electrochem. Soc.*, **153**, A997 (2006).
5. P. Piela, R. Fields and P. Zelenay, *J. Electrochem. Soc.*, **153**, A1902 (2006).
6. X. Ren, T. E. Springer and S. Gottesfeld, *J. Electrochem. Soc.*, **147**, 92 (2000).
7. J.-H. Choi, K.-W. Park, I.-S. Park, K. Kim, J.-S. Lee and Y.-E. Sung, *J. Electrochem. Soc.*, **153**, A1812 (2006).
8. H. F. Oetjen, V. M. Schmidt, U. Stimming and F. Trila, *J. Electrochem. Soc.*, **143**, 3838 (1996).
9. U. B. Demirci, *J. Power Sources*, **169**, 239 (2007).
10. G. J. K. Acres, *J. Power Sources*, **100**, 60 (2001).
11. S. Gamburzev and A. J. Appleby, *J. Power Sources*, **107**, 5 (2002).

12. S. Ha, C. Rice, R. I. Masel and A. Wieckowski, *J. Power Sources*, **112**, 655 (2002).
13. W. S. Jung, J. H. Han and S. Ha, *J. Power Sources*, **173**, 53 (2007).
14. S. Ha, R. Larsen and R. I. Masel, *J. Power Sources*, **144**, 28 (2005).
15. C. M. Misse, W. S. Jung, K. J. Jeong, J. K. Lee, J. Lee, J. H. Han, S. P. Yoon, S. W. Nam, T. H. Lim and S. A. Hong, *J. Power Sources*, **162**, 532 (2005).
16. K. Chu, M. A. Shannon and R. I. Masel, *J. Electrochem. Soc.*, **153**, A1562 (2006).
17. X. Xia and T. J. Iwasita, *J. Electrochem. Soc.*, **140**, 2559 (1993).
18. H. Yang and T. S. Zhao, *Electrochim. Acta*, **50**, 3243 (2004).
19. H. Qiao, H. Shiroishi and T. Okada, *Electrochim. Acta*, **53**, 59 (2007).
20. I.-M. Hsing, X. Wang and Y.-J. Leng, *J. Electrochem. Soc.*, **149**, A615 (2002).
21. R. Jiang, H. R. Kunz and J. M. Fenton, *J. Electrochem. Soc.*, **152**, A1329 (2005).
22. S. Ha, Z. Dunbar and R. I. Masel, *J. Power Sources*, **130**, 129 (2003).
23. R. Larsen, S. Ha, J. Zakzeski and R. I. Masel, *J. Power Sources*, **157**, 78 (2006).
24. R. O'Hayre, S. W. Cha, W. Colalla and F. B. Frinz, *Fuel cell fundamentals*, Wiley, New York, 145 (2006).
25. Y. Zhu, Z. Kahn and R. I. Masel, *J. Power Sources*, **139**, 15 (2005).
26. R. Benítez, J. Soler and L. Daza, *J. Power Sources*, **151**, 108 (2005).
27. O. A. Baturina and G. E. Wnek, *Electrochem. Solid-State Lett.*, **8**, A267 (2005).
28. G. Li, and P. G. Pickup, *J. Electrochem. Soc.*, **150**, C745 (2003).
29. H. J. Choi, J. Kim, Y. Kwon and J. H. Han, *J. Power Sources*, **195**, 160 (2010).
30. Z. Xie, T. Navessin, K. Shi, R. Chow, Q. Wang, D. Song, B. Andreaus, M. Eikerling, Z. Liu and S. Holdcroft, *J. Electrochem. Soc.*, **152**, A1171 (2005).
31. J. H. Choi, K. J. Jeong, Y. Dong, J. H. Han, T. H. Im, J. S. Lee and Y. E. Sung, *J. Power Sources*, **163**, 71 (2006).
32. M. Lukaszewski, K. Kusmierczyk, J. Kotowski, H. Siwek and A. Czerwinski, *J. Solid State Electrochem.*, **7**, 69 (2003).